Cell Stress and Chaperones (2025) 30:130–142
https://doi.org/10.1016/j.cstres.2025.03.002

Lycium barbarum polysaccharide alleviates H_2O_2-induced premature senescence by downregulating miRNA-34a-5p in ARPE-19 cells

Meng Kong[1,2] · Jingwen Li[2,1] · Rong Jin[3,2] · Yi Zhang[2,1] · Jia You[2,4] · Nan Wang[2,1] · Nianting Tong[2,1,*]

Received: 18 February 2025 / Revised: 12 March 2025 / Accepted: 14 March 2025

Abstract

The premature senescence of retinal pigment epithelium (RPE) plays a significant role in the development of age-related macular degeneration. This study aimed to investigate the potential protective effect of *Lycium barbarum* polysaccharide (LBP) against H_2O_2-induced premature senescence and to elucidate the underlying mechanisms. The ARPE-19 cell line was subjected to H_2O_2 exposure to create a model of premature senescence. The modulation of microRNA-34a-5p expression was accomplished using antagomir and agomir, as assessed by quantitative real-time polymerase chain reaction. The senescence model was successfully established by treating cells with 200 μM H_2O_2 for 2 hours daily over a span of three consecutive days. This oxidative stress resulted in a notable increase in the proportion of senescence-associated beta-galactosidase-positive cells, reaching 33.5%, without significant alterations in cell viability or apoptosis. In the ARPE-19 cells undergoing premature senescence, there was a marked increase in reactive oxygen species (ROS) production and malondialdehyde levels, coupled with a significant decrease in the activity of total superoxide dismutase, glutathione peroxidase, and catalase. Additionally, microRNA-34a-5p was found to be overexpressed in these cells. Treatment with LBP alleviated H_2O_2-induced premature senescence, diminished the overexpression of microRNA-34a-5p, and suppressed ROS production. Moreover, the incubation with ago-34a reversed the protective effect of LBP in ARPE-19 cells. In conclusion, the overexpression of microRNA-34a-5p contributes to the H_2O_2-induced premature senescence of ARPE-19 cells. LBP appears to mitigate this premature senescence, at least in part, by downregulating microRNA-34a-5p expression and reducing oxidative stress.

Keywords Premature senescence · Retinal pigment epithelium · Lycium barbarum polysaccharide · MicroRNA-34a-5p · Oxidative stress

Introduction

Age-related macular degeneration (AMD) is a predominant cause of visual impairment among individuals aged over 50 years.[1] A systematic review and meta-analysis indicated that the global population affected by AMD was approximately 196 million in 2020, with projections suggesting an increase to 288 million by 2040;

Abbreviations: AMD, age-related macular degeneration; ATP, adenosine triphosphate; CAT, catalase; CCK-8, cell counting kit-8; CNV, choroidal neovascularization; DCFH DA, 2',7' dichlorodihydrofluorescein diacetate; GA, geographic atrophy; GSH-px, glutathione peroxidase; HBSS, Hank's Balanced Salt Solution; LBP, Lycium barbarum polysaccharide; MDA, malondialdehyde; miRNAs, microRNAs; miR-34a, microRNA-34a; PBS, phosphate-buffered saline; qPCR, quantitative real-time polymerase chain reaction; ROS, reactive oxygen species; RPE, retinal pigment epithelium; SA β gal, senescence-associated beta-galactosidase; SD, standard deviation; SOD, superoxide dismutase

* Nianting Tong
drtongnt@qdu.edu.cn

[1] School of Medicine, Qingdao University, 266001, Qingdao, China

[2] Department of Ophthalmology, Qingdao Municipal Hospital, 266001, Qingdao, China

[3] Department of Pediatrics, Affiliated Hospital of Qingdao University, 266001, Qingdao, China

[4] Department of Ophthalmology, Qingdao Central Hospital, 266001, Qingdao, China.

Published online: 18 March 2025

thereby, the burden of this condition is significant.[2] Clinically, AMD is categorized by stage, ranging from early (characterized by the presence of medium-sized drusen and retinal pigmentary alterations) to late stages (classified as either neovascular [wet AMD] or atrophic [dry AMD]).[3] In the early stages, AMD is typically marked by pigmentary irregularities and the accumulation of extracellular material known as drusen at the retinal pigment epithelium (RPE)-choroidal interface. Drusen are classified by size as small (≤63 mm), intermediate (> 63 mm but < 125 mm), or large (≥125 mm).[4] As AMD progresses to the intermediate stage, the risk of advancing to late or advanced AMD increases due to the presence of extensive and confluent drusen.[5] Statistically, approximately half of the individuals with significant macular drusen will progress to vision-threatening conditions such as geographic atrophy or neovascularization within 5 years.[6] Geographic atrophy, characterized by extensive loss of RPE cells, is a defining feature of dry AMD, whereas wet AMD, also referred to as neovascular AMD, is marked by choroidal neovascularization, characterized by the formation of new, abnormal blood vessels from the choroid into the sub-retinal and sub-RPE areas, ultimately leading to rapid and severe vision loss.[7] Understanding these distinct manifestations is crucial for therapeutic interventions.[8] Although the complete pathogenesis for AMD remains elusive, it is recognized as a slowly progressive multifactorial condition characterized by genetic anomalies and environmental factors.[9,10]

The onset of AMD is often insidious; thus, by the time patients become aware of a notable deterioration in their vision and experience metamorphopsia, the lesions have typically reached an advanced stage. Currently, there are no effective pharmacological treatments available for AMD, particularly for geographic atrophy associated with dry AMD, due to the unclear mechanisms governing the progression of the disease. Most research regarding oxidative stress and AMD has primarily concentrated on elucidating how oxidative stress triggers apoptosis in RPE cells. However, it is uncommon to observe widespread RPE cell death in the early stages of AMD. It is plausible that cellular senescence in RPE may arise as a consequence of alterations in response to oxidative stress during the early phase of AMD.

Aging diminishes the capacity to react and adapt to the cumulative effects of various exposures, leading to age-related disease when cellular dysfunction in compromised cytoprotective pathways becomes sufficiently severe to instigate tissue damage.[11] RPE senescence, classified as an age-related condition, plays a significant role in the pathogenesis of AMD.[12–14] Previous studies have also indicated a correlation between oxidative stress and RPE senescence,[15–17] with antioxidant agents demonstrating the ability to alleviate this senescence.[14,18,19]

MicroRNAs (miRNAs), which are small (~20–24-nucleotide) noncoding RNA molecules, play crucial roles in post-transcriptional gene regulation and the modulation of both physiological and pathological cellular processes.[20] Previous research has highlighted substantial alterations in miRNA expression within the retinal tissues of AMD patients, suggesting that miRNAs may contribute to the pathological mechanisms of AMD by targeting specific downstream transcription factors.[21] In our earlier investigation,[22] we assessed the expression levels of miR-34a in the vitreous humor of young and old patients without AMD, as well as those with AMD. Our findings revealed elevated miR-34a levels in AMD patients, with a significant positive correlation between the miR-34a expression and age, indicating its potential involvement in RPE aging and AMD pathogenesis.

Lycium barbarum polysaccharide (LBP) is a renowned traditional Chinese herbal medicine, recognized for its extensive range of biological activities, including anti-inflammatory,[23–25] antioxidant,[26–29] and anti-aging properties.[30–33] Several previous studies have reported that LBP can significantly reduce oxidative stress and inhibit cellular senescence in various experimental models. For example, in different cell types and animal models, LBP treatment has been shown to decrease reactive oxygen species (ROS) levels, restore mitochondrial function, mitigate DNA damage, and improve antioxidant enzyme activities, thereby delaying the onset of cellular senescence.[33–38] A recent systematic review[39] highlighted LBP's capacity to reduce oxidative stress, restore mitochondrial functionality, mitigate DNA damage, and inhibit cellular senescence across both *in vitro* and *in vivo* aging models. Despite these encouraging findings, the specific inhibitory action of LBP on oxidative stress-induced premature senescence in RPE cells has not yet been explored.

The present study was, therefore, designed to address this gap by investigating whether LBP can alleviate H_2O_2-induced premature senescence in ARPE-19 cells, with a focus on its modulation of miRNA34a-5p expression.

Results

Effects of various LBP concentrations on ARPE-19 cells

ARPE-19 cells were cultured for 3 days with varying concentrations of LBP, after which cell viability and apoptosis were assessed. Figure 1(a) shows that LBP at 25 to 200 μg/mL was nontoxic, but viability decreased significantly as the LBP concentration increased to 400 μg/

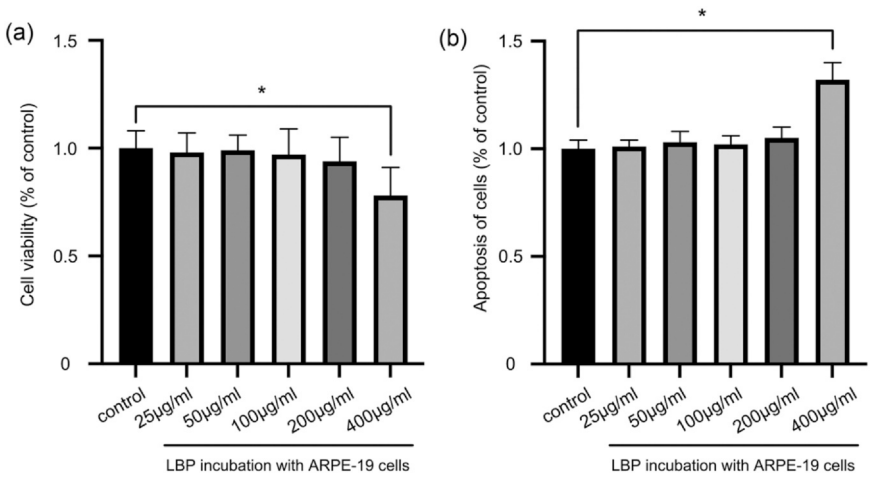

Fig. 1 Cell viability and the extents of apoptosis after 3 days incubation with LBP at different concentrations. (a) No significant decrease in cell viability was evident until the LBP concentration reached 400 μg/mL. (b) The extent of apoptosis was comparable to the extent in the control group at LBP concentrations from 25 to 200 μg/mL; apoptosis increased significantly as the LBP concentration further increased to 400 μg/mL. Abbreviation used: LBP, *Lycium barbarum* polysaccharide.

mL. The apoptosis trend was similar. Therefore, we used LBP at 200 μg/mL in the following experiments.

Three-day H_2O_2 exposure induces premature senescence in ARPE-19 cells without inducing apoptosis

To model premature senescence in ARPE-19 cells, H_2O_2 was introduced to the culture medium at a sublethal concentration of 200 μM, as described above. The senescence, viability, and apoptosis of ARPE-19 were observed from baseline to 5 days after the oxidative stimuli. The changes in ARPE-19 cell morphology are shown in Figure 2(a). The proportion of SA-β-gal-positive cells exhibited a significant time-dependent increase, rising from negligible levels at baseline to 19.1%, 27.3%, 33.5%, and 36.8% at 1, 2, 3, and 5 days, respectively, after the H_2O_2 intervention. A significant difference from the control group was found on the first day after oxidative stimuli (Figure 2(b) and (c)). The situation was similar in the annexin-V/FITC double staining study: in the first 3 days, there was no notable increase in cell apoptosis compared to either baseline or the control group; however, it increased significantly to 41.3% 5 days after the stimuli, which was markedly higher than the control group (4.9%, $p < 0.05$; Figure 2(d) and (e)). No

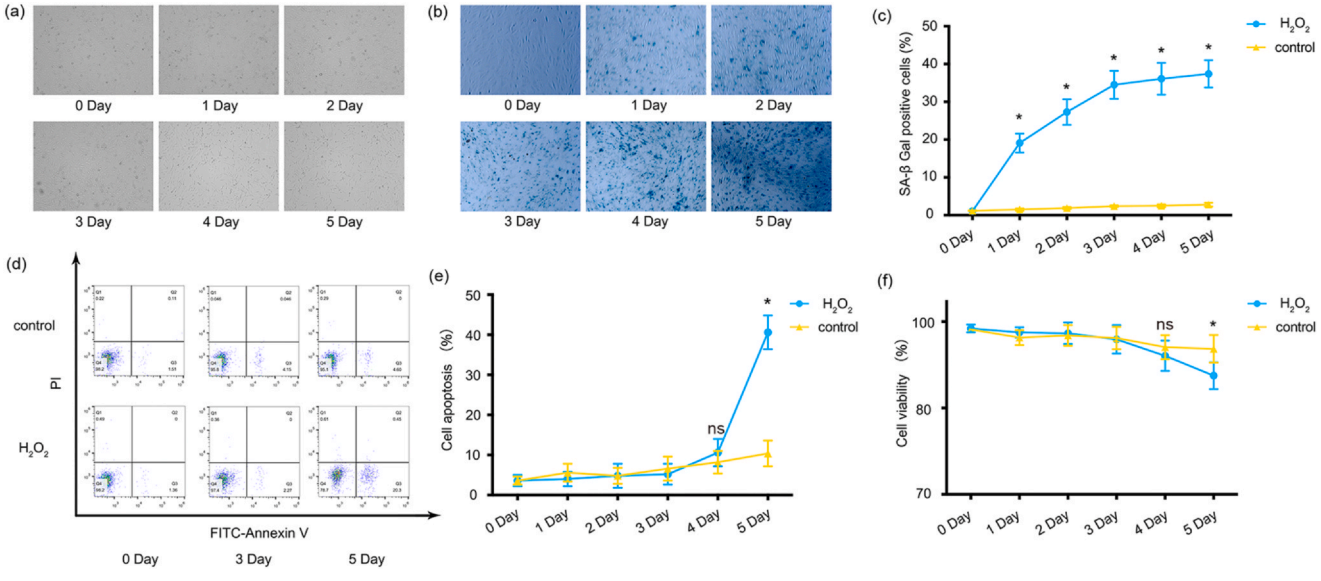

Fig. 2 H_2O_2 induces premature senescence in ARPE-19 cells. (a) Morphological changes in ARPE-19 cells during incubation with H_2O_2 from baseline to day 5. SA-β-Gal staining was used to detect senescence in ARPE-19 cells. (b) Representative images of SA-β-Gal-stained ARPE-19 cells, illustrating the qualitative senescent phenotype, after incubation with H_2O_2 for 5 days. (c) Quantification of SA-β-Gal-stained ARPE-19 cells. (d) Representative Annexin-V/PI-stained images of APRE-19 cells. (e) Quantification of ARPE-19 cell apoptosis. (f) ARPE-19 cell viability as measured by the CCK-8 assay. All experiments were repeated six times; ns represents $P > 0.05$, and * represents $P < 0.05$ compared to the control.

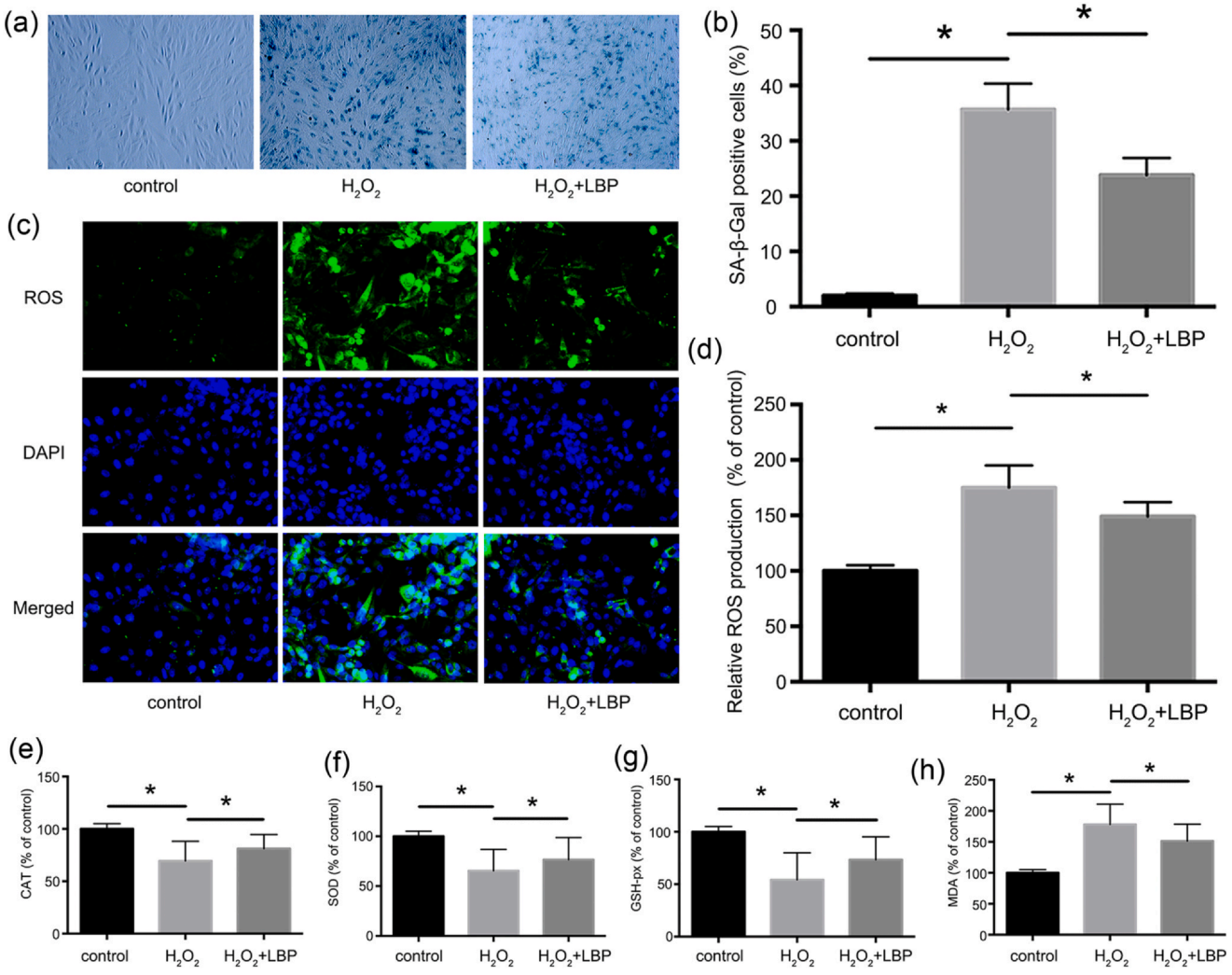

Fig. 3 LBP alleviated H_2O_2-induced premature senescence and improved the redox system status in ARPE-19 cells. (a) SA-β-Gal staining of H_2O_2-treated ARPE-19 cells exposed or not to LBP. (b) Quantification of SA-β-Gal-stained ARPE-19 cells in different groups. (c) Representative images of ROS accumulation in different groups of ARPE-19 cells. (d) Quantification of ROS levels. (e-h) Levels of CAT, GSH-px, SOD, and MDA in different groups. All experiments were repeated six times; *$P < 0.05$ for comparisons of group means. Abbreviations used: LBP, *Lycium barbarum* polysaccharide; CAT, catalase; GSH-px, glutathione peroxidase; SOD, superoxide dismutase; MDA, malondialdehyde.

significant difference in cell viability was evident until 3 days after oxidative stimulation; the viability was 87.5% at 5 days, significantly lower than in the control group (94.1%, $p < 0.05$; Figure 2(f)). These findings indicated that a premature senescence model in ARPE-19 cells could be effectively established incubating the cells with H_2O_2 at a concentration of 200 μM for 3 days, and this model was used in the following study.

LBP reduces ROS aggregation, ameliorates the status of the redox system, and alleviates H_2O_2-induced premature senescence in ARPE-19 cells

Three days after H_2O_2 stimuli, the SA-β-gal-positive cell proportion was significantly greater than that observed in the control group (36.5% vs. 2.6%, $P < 0.05$). The treatment with LBP notably counteracted the increase in SA-β-gal-positive cells, reducing their proportion to 25.7% ($P < 0.05$) in comparison to H_2O_2 stimuli group (Figure 3(a) and (b)). Notably, there was no significant increase in SA-β-gal-positive cells observed following LBP pretreatment in the absence of H_2O_2 stimulation (Figure S1).

To assess oxidative stress responses within the cells, we evaluated cellular ROS production, lipid peroxidation levels, and the activity of various intrinsic antioxidant enzymes. The H_2O_2-induced premature senescence resulted in a significant accumulation of ROS, reaching 172.37% of the control group ($P < 0.05$) (Figure 3(c) and (d)). Simultaneously, the activity levels of catalase (CAT), glutathione peroxidase (GSH-px), and superoxide dismutase (SOD)

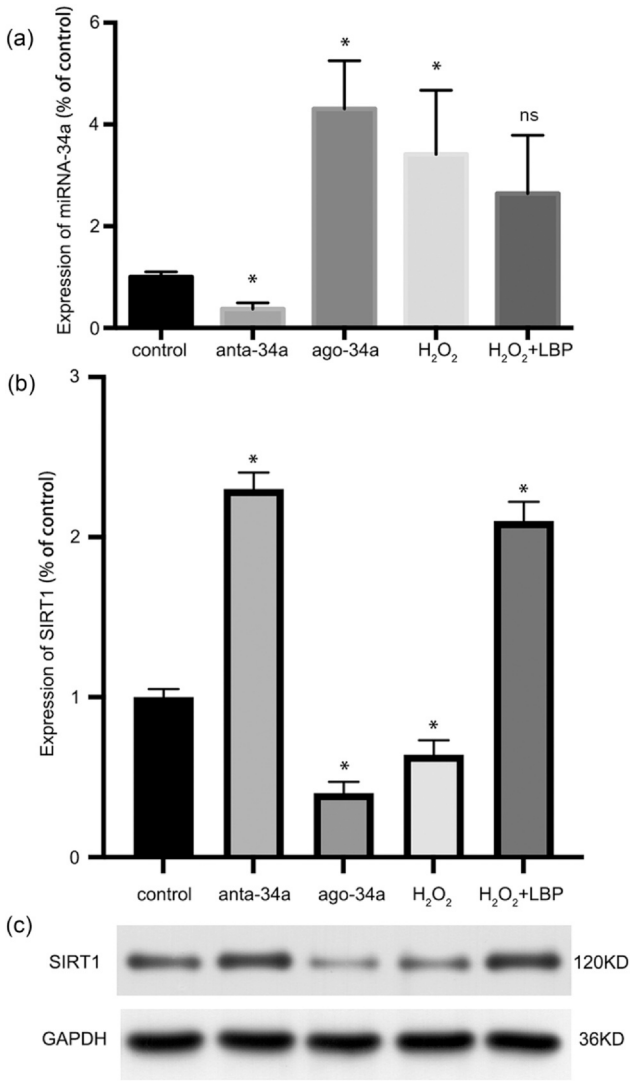

Fig. 4 Expression levels of miRNA-34a-5p and SIRT1 in ARPE-19 cells under various conditions. (a) The miRNA-34a-5p level significantly decreased and increased (compared to the control group) after incubation with anta-34a and ago-34a, respectively. (b) In H_2O_2-treated prematurely senescent ARPE-19 cells, the expression of SIRT1 decreased significantly, while LBP pretreatment mitigated this decrease. All experiments were repeated six times; ns represents $P > 0.05$, and $^*P < 0.05$ compared to the control. (c) Representative images of Western blots used to derive SIRT1 expression levels.

decreased significantly to 71.2%, 54.6%, and 69.3% of the control group, respectively ($P < 0.05$), while the malondialdehyde (MDA) level in the H_2O_2 group increased significantly to 182% of the control group ($P < 0.05$) (Figure 3(e)–(h)). These findings indicate that oxidative stress plays a critical role in the senescence of ARPE-19 cells induced by H_2O_2. However, LBP significantly inhibited ROS accumulation and reduced ROS production to 149.71% relative to the control group, which was significantly different compared to the H_2O_2 stimuli group ($P < 0.05$) (Figure 3(c) and (d)). Also, the activity levels of CAT, GSH-px, and SOD increased significantly to 85.7%, 77.3%, and 78.1% of the control group, respectively, which were all significantly different compared to the H_2O_2 stimuli group ($P < 0.05$) (Figure 3(e)–(g)). Accordingly, the MDA level decreased significantly to 156.3% of the control group, which was significantly different compared to the H_2O_2 stimuli group ($P < 0.05$) (Figure 3(h)). These results underscore that LBP treatment can ameliorate oxidative stress in ARPE-19 and, consequently, mitigate cell senescence.

LBP downregulates the expression of miRNA-34a-5p and suppresses SIRT1 downregulation in ARPE-19 cells induced by H_2O_2 stimulation in the premature senescence model

In the context of regulating miRNA-34a-5p expression, we employed a specific inhibitor (antagomir) and activator (agomir) for miRNA-34a-5p (anta-34a and ago-34a, respectively), which were transfected into ARPE-19 cells, as mentioned above. The numbers of SA-β-gal-positive cells did not increase significantly after incubation with anta-34a or ago-34a in the absence of H_2O_2 stimulation (Figure S1). The effectiveness of anta-34a and ago-34a was confirmed through quantitative PCR, revealing no significant alteration in miRNA-34a-5p expression after incubation with either anta-NC or ago-NC, or after pretreatment with the transfection reagent Lipo2000 (Figure S2). The expression levels of miRNA-34a-5p were significantly reduced to 37.2% ($P < 0.05$) and elevated to 431.1% ($P < 0.05$) relative to the control group following treatment with anta-34a and ago-34a incubation (Figure 4(a)). These results demonstrate the capability of anta-34a and ago-34a to effectively modulate the expression of miRNA-34a-5p in ARPE-19 cells. Furthermore, it was observed that the expression of miRNA-34a-5p significantly increased in premature senescence ARPE-19 cells, reaching 340.8% of control levels. In contrast, LBP treatment significantly reversed this trend, reducing the expression of miRNA-34a-5p to 263.9% of the control group ($P < 0.05$ compared to the H_2O_2 stimuli group; Figure 4(a)).

Given that miR-34a inhibits SIRT1 expression post-transcriptionally, we confirmed an inverse correlation between SIRT1 levels and miRNA-34a-5p levels. Incubation with anta-34a and ago-34a led to respective upregulation and downregulation of SIRT1 expression. Hydrogen peroxide significantly inhibited SIRT1 expression but LBP pretreatment rescued this inhibition (Figure 4(b) and (c)).

LBP reduces ROS aggregation and mitochondrial ROS production by downregulating miRNA-34a-5p in ARPE-19 cells to alleviate H_2O_2-induced premature senescence

To explore the influence of miRNA-34a-5p on the premature senescence triggered by oxidative stress, ARPE-

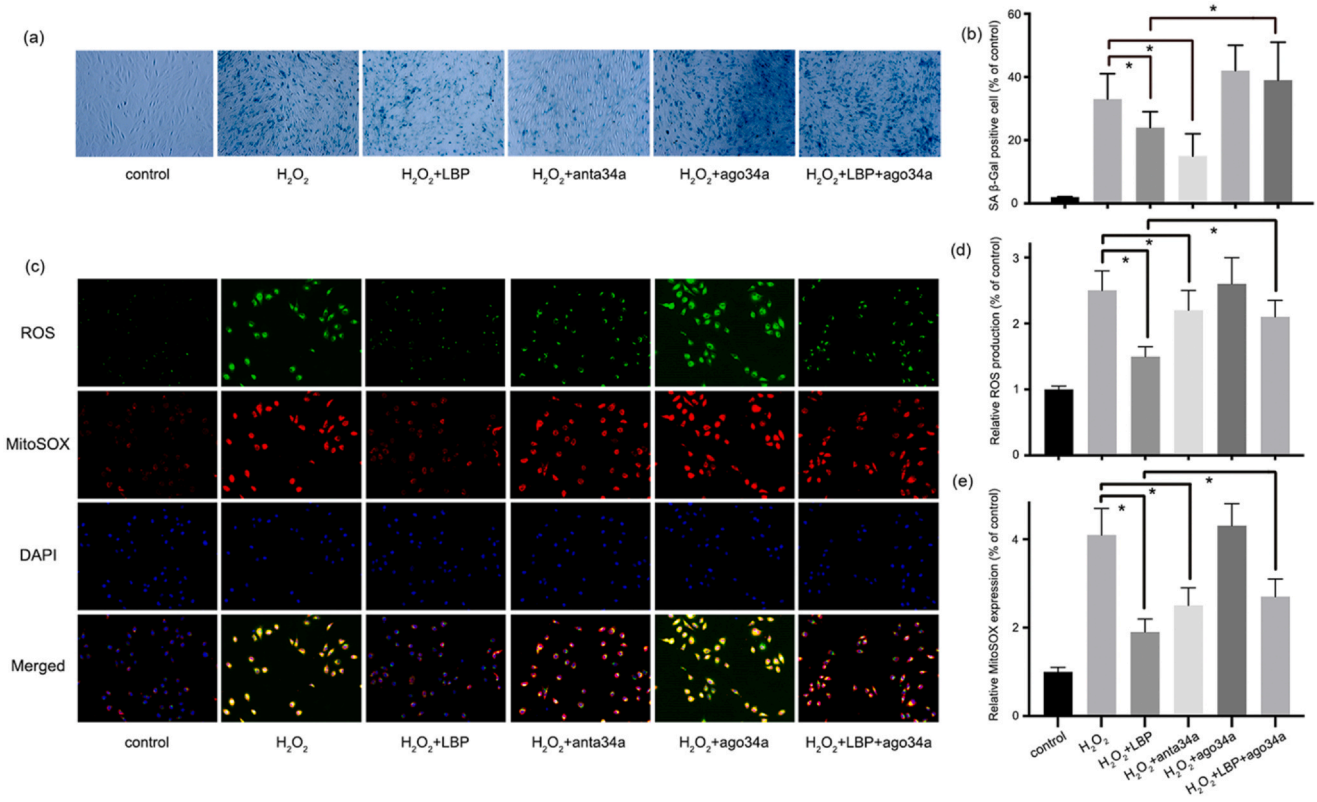

Fig. 5 Overexpression of miRNA-34a-5p during H_2O_2-induced premature senescence in ARPE-19 cells and LBP alleviation of senescence (at least partly *via* downregulation of miRNA-34a-5p expression). (a) Representative images of SA-β-Gal-stained ARPE-19 cells in different groups. (b) Quantification of SA-β-Gal-stained ARPE-19 cells in different groups. (c) Representative images of ROS accumulation and mitochondrial superoxide production in ARPE-19 cells in different groups. (d) Quantification of ROS production in different groups of ARPE-19 cells. (e) Quantification of MitoSOX in different groups of ARPE-19 cells. All experiments were repeated six times; * represents $P < 0.05$ for comparisons of group means. Abbreviations used: LBP, Lycium barbarum polysaccharide; ROS, reactive oxygen species.

19 cells subjected to H_2O_2 were incubated with anta-34a. Although H_2O_2 significantly increased the percentage of SA-β-gal-positive cells to 33.7% ($P < 0.05$), the downregulation of miRNA-34a-5p modulated by anta-34a significantly decreased the percentage of SA-β-gal-positive cells to 15.0% compared to the H_2O_2-treated group ($P < 0.05$; Figure 5(a) and (b)). Simultaneously, downregulation of miRNA-34a-5p significantly decreased ROS production to 212.9% and mitochondrial ROS production to 257.6% relative to the control group, which was significantly different compared to the H_2O_2 stimuli group (248.9% of control for ROS production, $P < 0.05$%, and 403.1% of control for mitochondrial ROS production; Figure 5(c) and (d)). These results demonstrate that overexpression of miRNA-34a-5p might contribute to H_2O_2-induced premature senescence, potentially through the promotion of ROS generation within the cytoplasm and mitochondria in ARPE-19 cells.

Although LBP treatment significantly reduced the proportion of SA-β-gal-positive cells to 24.1%, the upregulation of miRNA-34a-5p modulated by ago-34a significantly increased the proportion of SA-β-gal-positive cells to 39.2% compared to the LBP treatment group ($P < 0.05$; Figure 5(a) and (b)). Also, incubation with ago-34a reversed the inhibition of ROS accumulation in cytoplasm and mitochondria by LBP in the treatment group, such that the level increased from 142.0% relative to the control group to 201.3% in ROS production and increased from 193.2% relative to the control group to 257.8% in mitochondrial ROS production ($P < 0.05$; Figure 5(c)–(e)). These results demonstrate that LBP can mitigate premature senescence in H_2O_2-induced ARPE-19 cells, at least partially, by downregulating the expression of miRNA-34a-5p and ameliorating oxidative stress.

Discussion

Our findings substantiate that premature senescence in ARPE-19 cells can be instigated through exposure to 200 μM H_2O_2 for 2 h daily over 3 consecutive days. This level of oxidative stress was associated with a

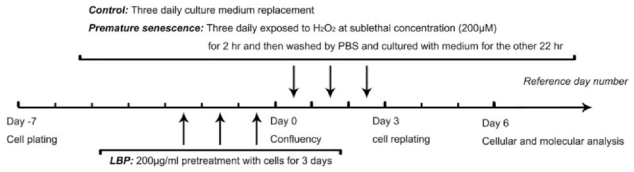

Fig. 6 Experimental design and the reference timeframe.

pronounced increase in the proportion of SA-β-gal-positive cells, while cell viability and apoptosis remained largely unchanged. However, a significant decline in cell viability, coupled with an increase in apoptosis, was observed 5 days post-H_2O_2 exposure. Therefore, we applied H_2O_2 treatment for 3 days to establish the model used in the consequent study. This model effectively illustrated the protective effects of LBP against oxidative stress-induced premature senescence. At the molecular level, we demonstrated that LBP likely confers its protective effect by downregulating miRNA-34a-5p expression and diminishing ROS production.

The RPE, characterized as a monolayer of polygonal and pigmented cells, is a distinctive epithelial structure located between the neural retina and Bruch membrane, adjacent to the fenestrated capillaries of the choriocapillaris.[49] RPE plays a critical role in the visual cycle and the maintenance of the outer retina. It is involved in the establishment of the blood-retinal barrier, protection against oxidative stress, nutrient transport and waste removal, ionic homeostasis, phagocytosis of photoreceptor outer segments, synthesis and release of growth factors, and the reisomerization of all-trans-retinal during the visual cycle, thereby contributing to the establishment of ocular immune privilege.[50] The senescence of RPE cells is implicated in the pathogenesis of various diseases, including AMD[51–53] and diabetic macular edema.[54–56] Previous investigations have employed a range of methodologies to treat ARPE-19 cells and develop a premature senescence model, utilizing agents such as *tert*-butyl hydroperoxide,[41] high glucose,[17] and pulsed H_2O_2 exposure.[57] In our study, we established the senescence model through H_2O_2 exposure in ARPE-19 cells, demonstrating that LBP mitigates the effects of H_2O_2-induced senescence.

In our experiments, H_2O_2 treatment led to a marked accumulation of ROS and a concomitant reduction in the activities of CAT, GSH-Px, and SOD. This redox imbalance is biologically significant because excessive ROS can damage lipids, proteins, and DNA, thereby accelerating cellular senescence. The diminished antioxidant capacity further impairs the cells' ability to counteract oxidative stress. In contrast, LBP treatment was able to partially restore the activities of these enzymes and reduce ROS levels. This restoration of redox balance not only mitigates oxidative damage but also enhances the overall cellular defense mechanisms, potentially delaying or preventing the progression of senescence-related phenotypes and contributing to cellular longevity. LBP, a prominent bioactive component extracted from goji berries, is extensively utilized in traditional Chinese medicine. They exhibit a range of beneficial effects, including antioxidant, anti-inflammatory, antiexcitotoxic, and anti-apoptotic activities. Consequently, LBP has garnered significant attention in the treatment of various ocular diseases, such as glaucoma, ischemia/reperfusion injury, AMD, retinitis pigmentosa, and diabetic retinopathy.[58] In an in vitro model of AMD, LBP demonstrated protective effects against amyloidβ oligomer-induced damage to ARPE-19, inhibiting both the oligomerization of amyloidβ and exhibiting anti-pyroptotic properties.[59] Moreover, a double-masked, randomized, placebo-controlled trial indicated that daily dietary inclusion of goji berries over 90days led to increased plasma antioxidant levels, while also safeguarding against hypopigmentation and the accumulation of soft drusen accumulation in the maculae of elderly individuals.[60]

Several previous studies have implicated miRNA-34a-5p as a critical mediator of cellular senescence and demonstrated that elevated levels of miRNA-34a-5p are associated with increased oxidative stress and senescence in various cell types.[61–63] Similarly, Maeda *et al.*[64] reported that miRNA-34a regulated Krüppel-like factor 4 expression is involved in hyperoxia-induced senescence in lung epithelial cells, thereby reinforcing the role of miRNA-34a in cellular aging processes. In contrast to these studies, our investigation not only confirms the role of miRNA-34a-5p in mediating H_2O_2-induced premature senescence in ARPE-19 cells but also identifies LBP as a potential therapeutic agent that modulates the expression of miRNA-34a-5p. This dual insight into both the mechanistic role of miRNA-34a-5p and the protective action of LBP underscores the novelty and potential significance of our findings.

Mitochondria play a pivotal role in meeting cellular energy demands by generating adenosine triphosphate through processes such as oxidative phosphorylation, the citric acid cycle, and β-oxidation. Mitochondrial dysfunction within the RPE has been identified as a critical contributor to the pathogenesis of AMD.[65–67] Additionally, mitochondria serve as both sources and targets of ROS.[68] Maintaining a dynamic equilibrium between the production and elimination of mitochondrial ROS is essential for regulating redox-mediated cell signaling pathways and preserving physiological function.[69] Disruption of this balance can lead to oxidative stress, resulting in cellular damage and pathological changes. Mitochondrial dysfunction is associated with impaired respiration, leading

to ROS accumulation,[70] while excessive ROS can inflict considerable damage to mitochondrial DNA, further aggravating mitochondrial dysfunction.[71,72] Previous studies proved that miRNA-34a-5p is related to cell senescence,[44,62,73] and factors regulating its expression can affect cellular senescence.[74–76] In addition, an age-related increase in miRNA-34a-5p expression has been observed in the posterior pole of murine eyes.[77] Our previous study found that miRNA-34a-5p is involved in age-related susceptibility to oxidative stress in ARPE-19 cells.[22] These findings underscore the significant involvement of miRNA-34a-5p in RPE senescence and dysfunction. In our current investigation, we observed an upregulation of miRNA-34a-5p within an H_2O_2-induced model of premature senescence, and inhibiting its expression through a specific antagonist markedly reversed the senescence of ARPE-19 cells. Besides, miRNA-34a-5p was identified as a crucial factor in high glucose-induced stress-associated premature senescence in retinal endothelial cells, mediated through mitochondrial dysfunction and diminished antioxidant capabilities.[44] Mechanistically, mitophagy impairment mediated by miRNA-34a-5p was found to be involved in the mitochondrial dysfunction in an in vivo model of liver injury induced by 2,2′,4,4′-Tetrabromodiphenyl ether.[78] In the present study, incubation with H_2O_2 caused significant ROS overloading and mitochondrial dysfunction in ARPE-19 cells. Following modulation of miRNA-34a-5p expression *via* pretreatment with anta-34a and ago-34a respectively, we noted substantial improvements in ROS overloading and mitochondrial dysfunction. This indicates a pivotal role of miRNA-34a-5p in mediating H_2O_2-induced ROS accumulation and mitochondrial dysfunction in ARPE-19 cells. These findings highlight the potential for mitigating RPE cell senescence and delaying the progression of AMD. Furthermore, pretreatment with LBP reversed the ROS overloading and mitochondrial dysfunction induced by H_2O_2, with this protective effect being significantly diminished when ARPE-19 cells were co-incubated with ago-34a. These results indicated that LBP might alleviate H_2O_2 induced premature senescence in ARPE-19 cells at least partly *via* inhibiting miRNA-34a-5p mediated ROS overloading and mitochondrial dysfunction.

SIRT1, an NAD-dependent histone deacetylase in mammals, is homologous to the yeast sir2 found in lower organisms. It is critically involved in numerous biological processes, including the regulation of the cell cycle, apoptosis, DNA repair, and gene silencing.[79] Furthermore, SIRT1 has been recognized for its protective roles against various human ailments, such as neurodegeneration diseases, cardiovascular diseases, metabolic syndromes, and tumorigenesis.[80] Additionally, SIRT1 has been implicated in the modulation of cellular senescence and organism longevity, primarily through the acetylation and deacetylation of specific substrates, thus influencing their transcriptional and enzymatic functions, as well as protein levels.[81] Bioinformatics analyses utilizing platforms such as pitcar, targetscan, Miranda, and microRNA.org have revealed that miRNA-34a-5p can specifically bind to the 3′ untranslated regions of SIRT1 mRNA. Empirical evidence across diverse tissues and cell types has confirmed that SIRT1 expression is regulated by miRNA-34a-5p, with the overexpression of miR-34a leading to a pronounced decrease in the post-transcriptional expression of SIRT1.[82–85] In our previous work, we identified an inverse relationship between SIRT1 and miRNA-34a-5p expression levels in ARPE-19 cells.[22] In the current study, the manipulation of miRNA-34a-5p expression *via* the application of anta-34a and ago-34a resulted in reciprocal changes in SIRT1 levels, suggesting a potential role for miRNA-34a-5p in H_2O_2 -induced premature senescence through its regulation of downstream SIRT1.

It is important to acknowledge some limitations of our study. Notably, our experiments were performed solely in vitro using ARPE-19 cells, which may not fully recapitulate the complex in vivo environment of the retina. In addition, while ARPE-19 cells are widely used as an RPE model, they have been increasingly scrutinized for their lack of key phenotypic characteristics of native RPE cells, suggesting that primary cultured RPE cells may provide a more accurate representation of in vivo conditions. Future studies incorporating in vivo models and primary RPE cells are warranted to validate these findings and to explore the translational potential of LBP as a therapeutic agent for AMD and other oxidative stress-related retinal diseases.

Conclusion

In conclusion, we established a model of premature senescence in ARPE-19 cells by exposing cells to 200 μM H_2O_2 for 2 h per day for 3consecutive days. Overexpression of miRNA-34a-5p was involved in the premature senescence of ARPE-19 cells induced by H_2O_2. LBP alleviated this senescence at least partly by downregulating miRNA-34a-5p expression.

Materials and methods

ARPE-19 cell culture

The human RPE cell line ARPE-19 (Procell Life Science and Technology Co, Ltd, Wuhan, China) was cultured following previously described protocols.[40] In brief, we maintained ARPE-19 cells under optimal conditions.

Cells were cultivated in Dulbecco's modified Eagle's medium/Nutrient Mixture F-12 supplemented with 10% fetal bovine serum (Dutscher, Brumath, France), along with 100 U/mL of penicillin and 100 mg/mL of streptomycin. The culture was maintained in a humidified environment containing 5% CO_2 at a temperature of 37 °C. For the experimental treatment, ARPE-19 cells were plated at a density of 35,000 cells/cm^2 and allowed to grow until reaching approximately 70% confluence under normoxia conditions, after which they were harvested for further analysis.

Model of oxidative stress-induced premature senescence

The concentration of 200 μM H_2O_2 was chosen based on prior literature and our preliminary experiments, which demonstrated that this dose induces premature senescence in ARPE-19 cells without significantly affecting cell viability or triggering apoptosis.[19,41] In brief, cells that reached 70% confluence after 7 days of culture were subjected to 200 μM H_2O_2 in a serum-free medium for 2 h each day over three consecutive days. After each treatment, the cells underwent three washed with phosphate-buffered saline (PBS) to eliminate any residual H_2O_2 and were subsequently cultured in the complete medium for 22 h. The cells were then replated and allowed to recover in complete culture medium (Dulbecco's modified Eagle's medium/Nutrient Mixture F-12 supplemented with 10% fetal bovine serum, 100 U/mL of penicillin, and 100 mg/mL of streptomycin) for 3 days before proceeding with subsequent experiments (Figure 6). It is noteworthy that during the H_2O_2 treatment, the culture medium was not changed, while routine culture involved daily medium renewal.

Preparation and treatment with LBP

The lyophilized powder of LBP, containing up to 95% polysaccharide, was procured from Shanghai Kang Zhou Funqi Polysaccharide Co, Ltd (Shanghai, China). For experimental applications, the lyophilized LBP powder was freshly dissolved in distilled water as previously described.[42] ARPE-19 cells were incubated with varying concentrations of LBP for 3 days, after which they were briefly washed with the medium before being exposed to hydrogen peroxide to trigger oxidative stress-induced premature senescence.

Senescence-associated beta-galactosidase staining for ARPE-19 senescence

Senescence-associated beta-galactosidase (SA-β-gal) staining was conducted utilizing a kit (C0602; Beyotime Biotechnology, Shanghai, China) in accordance with the manufacturer's guidelines.[43] Following collection, the ARPE-19 cells were washed three times with PBS, and fixed in 4% (w/v) paraformaldehyde for 15 min at room temperature. The fixation step was performed before the staining procedure. Subsequently, the fixed cells were incubated overnight at 37 °C in the absence of light with a working solution containing 0.05 mg/mL of 5-bromo-4-chloro-3-indolyl β-D-galactoside. After rinsing with PBS, the cells were examined microscopically for the development of blue coloration, and the percentage of SA-β-gal-positive cells was quantified from five random fields using ImageJ software (NIH, Bethesda, MD, USA).

Detection of ROS and redox status analysis

The intracellular levels of ROS were assessed using the fluorogenic probe, 2′,7′-dichlorodihydrofluorescein diacetate (DCFH-DA, S0033S, Beyotime, China), as previously detailed.[19] In brief, the cells were incubated at 37 °C in a medium containing 10 μM of DCFH-DA for 20 min, followed by two washes with PBS. The fluorescence emitted by DCFH-DA was then measured using a microscope or fluorescence-activated cell sorter, with excitation and emission wavelengths set at 485 and 522 nm, respectively.

To evaluate mitochondrial dysfunction, the production of mitochondrial superoxide was quantified utilizing MitoSOX Red (ThermoFisher, Waltham, MA, USA), a fluorescent probe specifically targeted to the mitochondria and selective for superoxide, as previously described.[44] A volume of 1 μL of MitoSOX Red was diluted in 999 μL of Hank's Balanced Salt Solution (HBSS) to prepare the MitoSOX Red solution for each well. ARPE-19 cells were incubated with MitoSOX Red solution for 60 min at 37 °C in the dark. Following staining, the cells were washed and resuspended in HBSS, and fluorescence was detected by a microscope or fluorescence-activated cell sorter, employing excitation and emission wavelengths of 488 nm and 525 nm, respectively.

Following various treatments, ARPE-19 cells were harvested to assess the level of MDA and the activities of total superoxide dismutase (SOD), glutathione peroxidase (GSH-px), and CAT utilizing commercially available assay kits (A003-4-1 for MDA, A001-3-1 for SOD, A005-1-1 for GSH-px, and A007-1-1 for CAT, Nanjing Jiancheng Bioengineering Institute, Nanjing, China) following the manufacturer's guidelines. All experimental procedures were replicated six times.

Assessment of ARPE-19 cell viability *via* cell counting Kit-8

The viability of ARPE-19 cells was evaluated using the Cell Counting Kit-8 (CCK-8, Beyotime, Shanghai,

China), adhering to the manufacturer's protocol.[45] Briefly, ARPE-19 cells were plated in 96-well plates at a density of 1×10^5 cells per well. After the treatment, 10 μL of the kit's working solution was introduced into each well and incubated for 2.5 h at 37 °C. The optical density was measured at 450 nm using a multifunctional microplate reader (BioTek, Synergy™ HTX, USA). All experiments were repeated six times. All experimental procedures were replicated six times.

Flow cytometry analysis of apoptosis in ARPE-19 cells

Flow cytometry was performed to assess ARPE-19 cell apoptosis, following previously established procedures.[46] In summary, the ARPE-19 cells were seeded in six-well plates at a density of 1×10^4 cells per well. After treatment, both adherent and suspended cells were collected and washed twice with cold PBS. Subsequently, cells were resuspended in binding buffer (1×10^5 cells per 100 μL) and stained with 5 μL of annexin-V–FITC and 5 μL of propidium iodide at room temperature in the dark. Following the addition of 500 μL of PBS, the stained cells were analyzed using a flow cytometer (FACSCalibur™ Flow Cytometer; BD Biosciences, San Jose, CA, USA), and the percentage of apoptotic cells was evaluated using FlowJo software (Tree Star, San Carlos, CA, USA). Each experiment was repeated six times.

Isolation of RNA and quantitative real-time polymerase chain reaction

Total RNA from cells was extracted using TRIzol (Invitrogen, Carlsbad, CA, USA) and subjected to a one-step phenol/chloroform/isoamyl alcohol extraction, following the manufacturer's instruction. A total of 500 ng of RNA was reverse transcribed into cDNA by incubating with 200 U of reverse transcriptase in a 10 μL reaction buffer at 37 °C for 1 h, utilizing a real-time kit (Takara Bio Inc, Shiga, Japan). Subsequently, 1 μL of cDNA served as a template for quantitative real-time polymerase chain reaction (qPCR). All gene transcripts were quantified using commercial reagents (Brilliant SYBR Green QPCR Master Mix; Agilent Technologies, Santa Clara, CA, USA) in conjunction with a qPCR system (7900HT; Applied Biosystems, Foster City, CA, USA). The relative levels of miRNA were normalized to the U6 expression level for each sample, and the expression level of each target gene was calculated using the formula $-2^{\Delta\Delta Ct}$.[47]

Construction and transfection of the antagomir and agomir of miRNA-34a-5p

Antagomir and agomir are specialized, chemically modified miRNAs, with antagomirs serving to inhibit endogenous miRNA expression, while agomir regulates the biological function of target genes by mimicking their endogenous counterparts. The sequences for antagomir-34a-5p (the inhibitor of miRNA-34a-5p) and its negative control (anta-NC) are 5′-ACAACCAGCUAAGACACUGCCA-3′ and 5′-CAGUACUUUUGUGUAGUACAA-3′, respectively. The sequences for agomir-34a-5p (which mimics miRNA-34a-5p) and its negative control (ago-NC), are 5′-UGGCAGUGUCUUAGCUGGUUGU-3′ and 5′-UUGUACUACACAAAAGUACUG-3′.

ARPE-19 cells were transfected with either 25 nM of the miRNA mimic or 50 nM of miRNA inhibitor using lipofectamine 2000 (Invitrogen) in conjunction with Opti-MEM, resulting in a reduced serum environment (Invitrogen). The cells were treated with the transfection complexes for a duration of 12 h to facilitate optimal absorption of the miRNA constructs, as recommended by the manufacturer's protocol.[48] Following the transfection process, the cells were cultured for an additional 12 h prior to exposure to oxidative stress or other experimental protocols.

Western blot analysis

Total protein was extracted from ARPE-19 cells utilizing ice-cold RIPA lysis buffer (Beyotime, Shanghai, China). Equal volumes of protein samples were subjected to 10% SDS-PAGE (Beyotime, Shanghai, China), subsequently transferred to 0.22 μm PVDF membranes (Millipore, Temecula, CA), and then blocked with 5% non-fat milk. The membranes were thereafter incubated with specific primary antibodies. The primary antibodies employed in this study included SIRT1 (Abcam, USA, 1:1000) and GAPDH (Abcam, USA, 1:5000). The ECL detection system (Millipore, Temecula, CA) was utilized to visualize the immunoreactive bands, with GAPDH serving as the control. Quantification of the gray values of protein bands was performed using ImageJ software (NIH, Bethesda, MD, USA).

Statistical analyses

All data are presented as mean ± standard deviation (SD); n represents the number of independent experiments conducted. The Mann–Whitney U test was utilized for the analysis of two independent samples, which pertains to figures where only two groups are compared. Conversely, the Kruskal-Wallis test was

employed for multi-group comparisons, as seen in figures where more than two groups were analyzed, with $p < 0.05$ deemed statistically significant.

Funding and support This study was supported by the National Natural Science Foundation of China (grant no. 81801381).

CRediT authorship contribution statement **Tong Nianting:** Supervision, Funding acquisition, Conceptualization. **Wang Nan:** Visualization, Validation, Software. **You Jia:** Investigation, Data curation. **Zhang Yi:** Visualization, Validation, Supervision, Formal analysis. **Jin Rong:** Validation, Software, Resources, Formal analysis. **Li Jingwen:** Resources, Methodology, Formal analysis, Data curation. **Meng Kong:** Writing – original draft, Methodology, Formal analysis.

Author contributions N.T. contributed to study conception and design. Materials were prepared and data were collected by all authors. N.T., M.K., J.L., R.J., and J.Y. analyzed/interpreted the results. N.T., M.K., Y.Z., and J.L. wrote the draft. J.L. and Y.Z. performed the staining of mitochondria in connection with oxidative stress staining and helped N.T. to amend the manuscript. All authors have read and approved the final manuscript.

Declarations of interest

No author has any commercial or financial relationship that could be construed as a potential conflict of interest.

Data availability statement

The data that have been used are confidential.

Acknowledgments We thank Textcheck (www.textcheck.com) for English language editing.

Appendix A. Supplementary data

Supplementary data associated with this article can be found online at doi:10.1016/j.cstres.2025.03.002.

References

1. Fleckenstein M, Keenan TDL, Guymer RH, et al. Age-related macular degeneration. *Nat Rev Dis Primers.* 2021;7:31.
2. Wong WL, Su X, Li X, et al. Global prevalence of age-related macular degeneration and disease burden projection for 2020 and 2040: a systematic review and meta-analysis. *Lancet Glob Health.* 2014;2:e106–e116.
3. Mitchell P, Liew G, Gopinath B, Wong TY. Age-related macular degeneration. *Lancet.* 2018;392:1147–1159.
4. Age-Related Eye Disease Study Research G. Risk factors associated with age-related macular degeneration. A case-control study in the age-related eye disease study: age-related eye disease study report number 3. *Ophthalmology.* 2000;107:2224–2232.
5. Age-Related Eye Disease Study Research G. A randomized, placebo-controlled, clinical trial of high-dose supplementation with vitamins C and E, beta carotene, and zinc for age-related macular degeneration and vision loss: AREDS report no. 8. *Arch Ophthalmol.* 2001;119:1417–1436.
6. Davis MD, Gangnon RE, Lee LY, et al. The Age-Related Eye Disease Study severity scale for age-related macular degeneration: AREDS Report No. 17. *Arch Ophthalmol.* 2005;123:1484–1498.
7. Kokotas H, Grigoriadou M, Petersen MB. Age-related macular degeneration: genetic and clinical findings. *Clin Chem Lab Med.* 2011;49:601–616.
8. Lambert NG, ElShelmani H, Singh MK, et al. Risk factors and biomarkers of age-related macular degeneration. *Prog Retin Eye Res.* 2016;54:64–102.
9. Rohrer B, Bandyopadhyay M, Beeson C. Reduced metabolic capacity in aged primary retinal pigment epithelium (RPE) is correlated with increased susceptibility to oxidative stress. *Adv Exp Med Biol.* 2016;854:793–798.
10. Guymer RH, Campbell TG. Age-related macular degeneration. *Lancet.* 2023;401:1459–1472.
11. Jones DP. Redox theory of aging. *Redox Biol.* 2015;5:71–79.
12. Sun S, Cai B, Li Y, et al. HMGB1 and caveolin-1 related to RPE cell senescence in age-related macular degeneration. *Aging.* 2019;11:4323–4337.
13. Blasiak J. Senescence in the pathogenesis of age-related macular degeneration. *Cell Mol Life Sci.* 2020;77:789–805.
14. Chen SJ, Lin TB, Peng HY, et al. Cytoprotective potential of fucoxanthin in oxidative stress-induced age-related macular degeneration and retinal pigment epithelial cell senescence in vivo and in vitro. *Mar Drugs.* 2021;19:1–15.
15. Kaarniranta K, Kajdanek J, Morawiec J, Pawlowska E, Blasiak J. PGC-1alpha protects RPE cells of the aging retina against oxidative stress-induced degeneration through the regulation of senescence and mitochondrial quality control. The significance for AMD pathogenesis. *Int J Mol Sci.* 2018;19:1–20.
16. Upadhyay M, Milliner C, Bell BA, Bonilha VL. Oxidative stress in the retina and retinal pigment epithelium (RPE): role of aging, and DJ-1. *Redox Biol.* 2020;37:101623.
17. Chen Q, Tang L, Xin G, et al. Oxidative stress mediated by lipid metabolism contributes to high glucose-induced senescence in retinal pigment epithelium. *Free Radic Biol Med.* 2019;130:48–58.
18. Sreekumar PG, Ishikawa K, Spee C, et al. The mitochondrial-derived peptide humanin protects RPE cells from oxidative stress, senescence, and mitochondrial dysfunction. *Invest Ophthalmol Vis Sci.* 2016;57:1238–1253.
19. Zhuge CC, Xu JY, Zhang J, et al. Fullerenol protects retinal pigment epithelial cells from oxidative stress-induced premature senescence via activating SIRT1. *Invest Ophthalmol Vis Sci.* 2014;55:4628–4638.
20. Dong H, Lei J, Ding L, Wen Y, Ju H, Zhang X. MicroRNA: function, detection, and bioanalysis. *Chem Rev.* 2013;113:6207–6233.
21. Ren C, Liu Q, Wei Q, et al. Circulating miRNAs as potential biomarkers of age-related macular degeneration. *Cell Physiol Biochem.* 2017;41:1413–1423.
22. Tong N, Jin R, Zhou Z, Wu X. Involvement of microRNA-34a in age-related susceptibility to oxidative stress in ARPE-19 cells by targeting the silent mating type information regulation 2 homolog 1/p66shc pathway: implications for age-related macular degeneration. *Front Aging Neurosci.* 2019;11:137.
23. Gao LL, Ma JM, Fan YN, et al. *Lycium barbarum* polysaccharide combined with aerobic exercise ameliorated non-alcoholic fatty liver disease through restoring gut microbiota, intestinal barrier and inhibiting hepatic inflammation. *Int J Biol Macromol.* 2021;183:1379–1392.

24. Wu Q, Liu LT, Wang XY, et al. *Lycium barbarum* polysaccharides attenuate kidney injury in septic rats by regulating Keap1-Nrf2/ARE pathway. *Life Sci.* 2020;242:117240.
25. Li W, Gao M, Han T. *Lycium barbarum* polysaccharides ameliorate intestinal barrier dysfunction and inflammation through the MLCK-MLC signaling pathway in Caco-2 cells. *Food Funct.* 2020;11:3741–3748.
26. Zhang F, Zhang X, Gu Y, et al. Hepatoprotection of Lycii Fructus polysaccharide against oxidative stress in hepatocytes and larval zebrafish. *Oxid Med Cell Longev.* 2021;2021:3923625.
27. Liu L, Sha XY, Wu YN, Chen MT, Zhong JX. *Lycium barbarum* polysaccharides protects retinal ganglion cells against oxidative stress injury. *Neural Regen Res.* 2020;15:1526–1531.
28. Varoni MV, Pasciu V, Gadau SD, et al. Possible antioxidant effect of *Lycium barbarum* polysaccharides on hepatic cadmium-induced oxidative stress in rats. *Environ Sci Pollut Res Int.* 2017;24:2946–2955.
29. Liu Y, Zhang Y. *Lycium barbarum* polysaccharides alleviate hydrogen peroxide-induced injury by up-regulation of miR-4295 in human trabecular meshwork cells. *Exp Mol Pathol.* 2019;106:109–115.
30. Gao Y, Wei Y, Wang Y, Gao F, Chen Z. *Lycium barbarum*: a traditional chinese herb and a promising anti-aging agent. *Aging Dis.* 2017;8:778–791.
31. Qi B, Ji Q, Wen Y, et al. *Lycium barbarum* polysaccharides protect human lens epithelial cells against oxidative stress-induced apoptosis and senescence. *PLoS One.* 2014;9:e110275.
32. Xia G, Xin N, Liu W, Yao H, Hou Y, Qi J. Inhibitory effect of *Lycium barbarum* polysaccharides on cell apoptosis and senescence is potentially mediated by the p53 signaling pathway. *Mol Med Rep.* 2014;9:1237–1241.
33. Zheng X, Wang J, Bi F, et al. Protective effects of *Lycium barbarum* polysaccharide on ovariectomyinduced cognition reduction in aging mice. *Int J Mol Med.* 2021;48:1–13.
34. Hu S, Liu D, Liu S, Li C, Guo J. *Lycium barbarum* polysaccharide ameliorates heat-stress-induced impairment of primary sertoli cells and the blood-testis barrier in rat via androgen receptor and Akt phosphorylation. *Evid Based Complement Alternat Med.* 2021;2021:5574202.
35. Tang R, Chen X, Dang T, et al. *Lycium barbarum* polysaccharides extend the mean lifespan of *Drosophila melanogaster*. *Food Funct.* 2019;10:4231–4241.
36. Zhang Z, Zhou Y, Fan H, et al. Effects of *Lycium barbarum* polysaccharides on health and aging of *C. elegans* depend on daf-12/daf-16. *Oxid Med Cell Longev.* 2019;2019:6379493.
37. Yang L, Gao Z, Lei L, et al. *Lycium barbarum* polysaccharide enhances development of previously-cryopreserved murine two-cell embryos via restoration of mitochondrial function and down-regulated generation of reactive oxygen species. *J Reprod Dev.* 2019;65:163–170.
38. Zhao R, Cai Y, Shao X, Ma B. Improving the activity of *Lycium barbarum* polysaccharide on sub-health mice. *Food Funct.* 2015;6:2033–2040.
39. Ni J, Au M, Kong H, Wang X, Wen C. *Lycium barbarum* polysaccharides in ageing and its potential use for prevention and treatment of osteoarthritis: a systematic review. *BMC Complement Med Ther.* 2021;21:212.
40. Yang J, Yang K, Meng X, Liu P, Fu Y, Wang Y. Silenced SNHG1 inhibited epithelial-mesenchymal transition and inflammatory response of ARPE-19 cells induced by high glucose. *J Inflamm Res.* 2021;14:1563–1573.
41. Glotin AL, Debacq-Chainiaux F, Brossas JY, et al. Prematurely senescent ARPE-19 cells display features of age-related macular degeneration. *Free Radic Biol Med.* 2008;44:1348–1361.
42. Yang YJ, Wang Y, Deng Y, et al. *Lycium barbarum* polysaccharides regulating miR-181/Bcl-2 decreased autophagy of retinal pigment epithelium with oxidative stress. *Oxid Med Cell Longev.* 2023;2023:9554457.
43. Zhang P, Wang Q, Nie L, et al. Hyperglycemia-induced inflamm-aging accelerates gingival senescence via NLRC4 phosphorylation. *J Biol Chem.* 2019;294:18807–18819.
44. Thounaojam MC, Jadeja RN, Warren M, et al. MicroRNA-34a (miR-34a) mediates retinal endothelial cell premature senescence through mitochondrial dysfunction and loss of antioxidant activities. *Antioxidants.* 2019;8:1–11.
45. Zhang D, Li H, Jiang X, et al. Role of AP-2alpha and MAPK7 in the regulation of autocrine TGF-beta/miR-200b signals to maintain epithelial-mesenchymal transition in cholangiocarcinoma. *J Hematol Oncol.* 2017;10:170.
46. Xu Y, Wang L, Cao L, Chen L, Liu Q. Involvement of NYD-SP15 in growth and oxidative-stress responses of ARPE-19. *J Cell Biochem.* 2018;120:1362–1375.
47. Cao Y, Wu TD, Wu H, et al. Synchrotron radiation micro-CT as a novel tool to evaluate the effect of agomir-210 in a rat spinal cord injury model. *Brain Res.* 2017;1655:55–65.
48. Chen X, Gu S, Chen BF, et al. Nanoparticle delivery of stable miR-199a-5p agomir improves the osteogenesis of human mesenchymal stem cells via the HIF1a pathway. *Biomaterials.* 2015;53:239–250.
49. Tarau IS, Berlin A, Curcio CA, Ach T. The cytoskeleton of the retinal pigment epithelium: from normal aging to age-related macular degeneration. *Int J Mol Sci.* 2019;20:1–19.
50. Ao J, Wood JP, Chidlow G, Gillies MC, Casson RJ. Retinal pigment epithelium in the pathogenesis of age-related macular degeneration and photobiomodulation as a potential therapy? *Clin Exp Ophthalmol.* 2018;46:670–686.
51. Dieguez HH, Romeo HE, Alaimo A, et al. Oxidative stress damage circumscribed to the central temporal retinal pigment epithelium in early experimental non-exudative age-related macular degeneration. *Free Radic Biol Med.* 2019;131:72–80.
52. Ferrington DA, Sinha D, Kaarniranta K. Defects in retinal pigment epithelial cell proteolysis and the pathology associated with age-related macular degeneration. *Prog Retin Eye Res.* 2016;51:69–89.
53. George SM, Lu F, Rao M, Leach LL, Gross JM. The retinal pigment epithelium: development, injury responses, and regenerative potential in mammalian and non-mammalian systems. *Prog Retin Eye Res.* 2021;85:100969.
54. Kuo C, Green CR, Rupenthal ID, Mugisho OO. Connexin43 hemichannel block protects against retinal pigment epithelial cell barrier breakdown. *Acta Diabetol.* 2020;57:13–22.
55. Beasley S, El-Sherbiny M, Megyerdi S, et al. Caspase-14 expression impairs retinal pigment epithelium barrier function: potential role in diabetic macular edema. *Biomed Res Int.* 2014;2014:417986.
56. Desjardins DM, Yates PW, Dahrouj M, Liu Y, Crosson CE, Ablonczy Z. Progressive early breakdown of retinal pigment epithelium function in hyperglycemic rats. *Invest Ophthalmol Vis Sci.* 2016;57:2706–2713.
57. Zhu W, Wu Y, Meng YF, et al. Effect of curcumin on aging retinal pigment epithelial cells. *Drug Des Devel Ther.* 2015;9:5337–5344.
58. Manthey AL, Chiu K, So KF. Effects of *Lycium barbarum* on the visual system. *Int Rev Neurobiol.* 2017;135:1–27.
59. Yang M, So KF, Lo ACY, Lam WC. The effect of *Lycium barbarum* polysaccharides on pyroptosis-associated amyloid beta1-40 oligomers-induced adult retinal pigment epithelium 19 cell damage. *Int J Mol Sci.* 2020;21:1–16.

60. Bucheli P, Vidal K, Shen L, et al. Goji berry effects on macular characteristics and plasma antioxidant levels. *Optom Vis Sci.* 2011;88:257–262.
61. Yu X, Zhang L, Wen G, et al. Upregulated sirtuin 1 by miRNA-34a is required for smooth muscle cell differentiation from pluripotent stem cells. *Cell Death Differ.* 2015;22:1170–1180.
62. Badi I, Burba I, Ruggeri C, et al. MicroRNA-34a induces vascular smooth muscle cells senescence by SIRT1 downregulation and promotes the expression of age-associated pro-inflammatory secretory factors. *J Gerontol A Biol Sci Med Sci.* 2015;70:1304–1311.
63. Bhattacharjee S, Zhao Y, Lukiw WJ. Deficits in the miRNA-34a-regulated endogenous TREM2 phagocytosis sensor-receptor in Alzheimer's disease (AD); an update. *Front Aging Neurosci.* 2014;6:116.
64. Maeda H, Yao H, Go H, Huntington KE, De Paepe ME, Dennery PA. Involvement of miRNA-34a regulated Kruppel-like factor 4 expression in hyperoxia-induced senescence in lung epithelial cells. *Respir Res.* 2022;23:340.
65. Terluk MR, Kapphahn RJ, Soukup LM, et al. Investigating mitochondria as a target for treating age-related macular degeneration. *J Neurosci.* 2015;35:7304–7311.
66. Brown EE, DeWeerd AJ, Ildefonso CJ, Lewin AS, Ash JD. Mitochondrial oxidative stress in the retinal pigment epithelium (RPE) led to metabolic dysfunction in both the RPE and retinal photoreceptors. *Redox Biol.* 2019;24:101201.
67. Fisher CR, Ferrington DA. Perspective on AMD pathobiology: a bioenergetic crisis in the RPE. *Invest Ophthalmol Vis Sci.* 2018;59:AMD41–AMD47.
68. Quintana-Cabrera R, Fernandez-Fernandez S, Bobo-Jimenez V, et al. gamma-Glutamylcysteine detoxifies reactive oxygen species by acting as glutathione peroxidase-1 cofactor. *Nat Commun.* 2012;3:718.
69. Dickinson BC, Chang CJ. Chemistry and biology of reactive oxygen species in signaling or stress responses. *Nat Chem Biol.* 2011;7:504–511.
70. King A, Gottlieb E, Brooks DG, Murphy MP, Dunaief JL. Mitochondria-derived reactive oxygen species mediate blue light-induced death of retinal pigment epithelial cells. *Photochem Photobiol.* 2004;79:470–475.
71. Karunadharma PP, Nordgaard CL, Olsen TW, Ferrington DA. Mitochondrial DNA damage as a potential mechanism for age-related macular degeneration. *Invest Ophthalmol Vis Sci.* 2010;51:5470–5479.
72. Kaarniranta K, Pawlowska E, Szczepanska J, Jablkowska A, Blasiak J. Role of mitochondrial DNA damage in ROS-mediated pathogenesis of age-related macular degeneration (AMD). *Int J Mol Sci.* 2019;20:1–18.
73. Zuccolo E, Badi I, Scavello F, et al. The microRNA-34a-Induced Senescence-Associated Secretory Phenotype (SASP) favors vascular smooth muscle cells calcification. *Int J Mol Sci.* 2020;21:1–17.
74. Guo Y, Li P, Gao L, et al. Kallistatin reduces vascular senescence and aging by regulating microRNA-34a-SIRT1 pathway. *Aging Cell.* 2017;16:837–846.
75. Zhang S, Zhang R, Qiao P, et al. Metformin-induced microRNA-34a-3p downregulation alleviates senescence in human dental pulp stem cells by targeting CAB39 through the AMPK/mTOR signaling pathway. *Stem Cells Int.* 2021;2021:6616240.
76. Xia W, Hou M. Mesenchymal stem cells confer resistance to doxorubicin-induced cardiac senescence by inhibiting microRNA-34a. *Oncol Lett.* 2018;15:10037–10046.
77. Smit-McBride Z, Forward KI, Nguyen AT, Bordbari MH, Oltjen SL, Hjelmeland LM. Age-dependent increase in miRNA-34a expression in the posterior pole of the mouse eye. *Mol Vis.* 2014;20:1569–1578.
78. Chen F, Feng L, Zheng YL, et al. 2, 2′, 4, 4′-tetrabromodiphenyl ether (BDE-47) induces mitochondrial dysfunction and related liver injury via eliciting miR-34a-5p-mediated mitophagy impairment. *Environ Pollut.* 2020;258:113693.
79. Vaziri H, Dessain SK, Ng Eaton E, et al. hSIR2(SIRT1) functions as an NAD-dependent p53 deacetylase. *Cell.* 2001;107:149–159.
80. Xie L, Huang R, Liu S, et al. A positive feedback loop of SIRT1 and miR17HG promotes the repair of DNA double-stranded breaks. *Cell Cycle.* 2019;18:2110–2123.
81. Chen C, Zhou M, Ge Y, Wang X. SIRT1 and aging related signaling pathways. *Mech Ageing Dev.* 2020;187:111215.
82. Wang Y, Zhou F, Li M, Zhang Y, Li N, Shao L. MiR-34a-5p promotes hepatic gluconeogenesis by suppressing SIRT1 expression. *Exp Cell Res.* 2022;420:113336.
83. Castro RE, Ferreira DM, Afonso MB, et al. miR-34a/SIRT1/p53 is suppressed by ursodeoxycholic acid in the rat liver and activated by disease severity in human non-alcoholic fatty liver disease. *J Hepatol.* 2013;58:119–125.
84. Fomison-Nurse I, Saw EEL, Gandhi S, et al. Diabetes induces the activation of pro-ageing miR-34a in the heart, but has differential effects on cardiomyocytes and cardiac progenitor cells. *Cell Death Differ.* 2018;25:1336–1349.
85. Marino MT, Grilli A, Baricordi C, et al. Prognostic significance of miR-34a in Ewing sarcoma is associated with cyclin D1 and ki-67 expression. *Ann Oncol.* 2014;25:2080–2086.